学位論文

Functional characterization of UBXN-6, a C-terminal cofactor of CDC-48, in *C. elegans*

（ CDC-48 の C 末端コファクターUBXN-6 の線虫における機能解析 ）

モジュンダー　シュモン
Mojumder Suman

熊本大学大学院医学教育部博士課程医学専攻
HIGOプログラム４年コース

指導教員

小椋　光　教授
熊本大学大学院医学教育部博士課程医学専攻分子細胞制御学

２０１９年 3 月

学　位　論　文

論文題名　:　Functional characterization of UBXN-6, a C-terminal cofactor of CDC-48, in *C. elegans*

（CDC-48 の C 末端コファクターUBXN-6 の線虫における機能解析）

著 者 名　:　モジュンダー　シュモン
Mojumder Suman

指導教員名　:　小椋　光　教授

審査委員名　:

分子生理学担当教授	富澤　一仁
微生物学担当教授	澤　智裕
染色体制御学担当准教授	石黒　啓一郎
損傷修復学担当講師	立石　智

２０１９年 3 月

Biochemical and Biophysical Research Communications 509 (2019) 462–468

Contents lists available at ScienceDirect

Biochemical and Biophysical Research Communications

journal homepage: www.elsevier.com/locate/ybbrc

Functional characterization of UBXN-6, a C-terminal cofactor of CDC-48, in *C. elegans*

Suman Mojumder [a, b], Rie Sawamura [a], Yuki Murayama [a], Teru Ogura [a, b], Kunitoshi Yamanaka [a, *]

[a] *Department of Molecular Cell Biology, Institute of Molecular Embryology and Genetics, Kumamoto University, 2-2-1 Honjo, Chuo-ku, Kumamoto, 860-0811, Japan*
[b] *Program for Leading Graduate Schools "HIGO Program", Kumamoto University, 1-1-1 Honjo, Chuo-ku, Kumamoto, 860-8556, Japan*

A R T I C L E I N F O

Article history:
Received 7 December 2018
Accepted 21 December 2018
Available online 27 December 2018

Keywords:
AAA ATPase
C. elegans
CDC-48/p97/VCP
CRISPR-Cas9
UBXN-6

A B S T R A C T

CDC-48 is a AAA (ATPases associated with diverse cellular activities) chaperone and participates in a wide range of cellular activities. Its functional diversity is determined by differential binding of a variety of cofactors. In this study, we analyzed the physiological role of a CDC-48 cofactor UBXN-6 in *Caenorhabditis elegans*. The amount of UBXN-6 was markedly increased upon starvation, but not with the treatment of tunicamycin and rapamycin. The induction upon starvation is a unique characteristic for UBXN-6 among C-terminal cofactors of CDC-48. During starvation, lysosomal activity is triggered for rapid clearance of cellular materials. We observed the lysosomal activity by monitoring GLO-1::GFP, a marker for lysosome-related organelles. We found that more puncta of GLO-1::GFP were observed in the *ubxn-6* deletion mutant after 12 h starvation compared with the wild-type strain. Taken together, we propose that UBXN-6 is involved in clearance of cellular materials upon starvation in *C. elegans*.

1. Introduction

CDC-48 (although it is also called VCP or p97 in mammals, we use CDC-48 throughout this study) is a AAA (ATPases associated with diverse cellular activities) chaperone and is involved in a wide variety of cellular processes, such as protein quality control, protein degradation, and organelle membrane fusion [1–4]. The functional diversity of CDC-48 is determined by differential binding of a variety of cofactors [5–7]. Several cofactors have been identified in *Caenorhabditis elegans*, e.g. NPL-4-UFD-1 and six different UBXN proteins, which bind to the N domain of CDC-48 [8], and UFD-2 and UFD-3, which bind to the C-terminal portion of CDC-48 [9]. In general, it is considered that N-terminal cofactors are involved in the selection of substrate proteins, whereas C-terminal cofactors may determine the fate of these substrate proteins [5–7]. It should be noted that two highly homologous CDC-48s, CDC-48.1 and CDC-48.2, exist in *C. elegans* and that their function is essential and redundant [10,11].

Human UBXD1 (UBXN-6 in *C. elegans*) has been reportedly involved in vesicle trafficking [12], endolysosomal sorting [13], autophagic clearance of damaged lysosome [14], outer mitochondrial membrane-associated degradation [15], and mitophagy [16]. UBXD1/UBXN-6 is unique among the cofactors of CDC-48, since it can interact with both the N domain and the C-terminal portion of CDC-48 through a bipartite binding mechanism [17,18]. UBXD1/UBXN-6 contains three remarkable domains: N, PUB, and UBX domains. The N and PUB domains of UBXD1/UBXN-6 bind to the N domain and the C-terminal portion of CDC-48, respectively [17,18]. The N domain of UBXD1 is important to recruit UBXD1 at the endosome in the endocytic pathway. The *in vitro* study showed that the N domain of UBXD1 regulates inter-domain communication within the CDC-48 hexamer and can reduce the ATPase activity of CDC-48, indicating the regulatory effect of UBXD1 on CDC-48 mediated cellular functions [19]. It is interesting to mention that the UBX domain of UBXD1/UBXN-6 does not participate in binding to the N domain of CDC-48 [18]. Recently, it has been shown that the UBX domain of UBXD1 exclusively mediates the translocation of UBXD1 to depolarized mitochondria and subsequently promotes mitochondrial recruitment of CDC-48 for accelerating mitophagy [16].

In this study, we created the *ubxn-6* deletion mutant and analyzed the physiological role of UBXN-6 in *C. elegans*. The amount

* Corresponding author.
E-mail address: yamanaka@gpo.kumamoto-u.ac.jp (K. Yamanaka).

https://doi.org/10.1016/j.bbrc.2018.12.155
0006-291X/

of UBXN-6 was specifically increased upon starvation. Together with microscopic analyses, we propose that UBXN-6 is involved in clearance of cellular materials upon starvation in *C. elegans*.

2. Materials and methods

2.1. C. elegans strains

Worms were maintained at 20 °C using standard protocols as described previously [20]. The Bristol strain N2 was used as the wild-type strain. The deletion mutants *cdc-48.1* (*tm544*), *cdc-48.2* (*tm659*), *ufd-2* (*tm1380*), and *ufd-3* (*tm2915*) were described previously [9,11]. The strain VS17 *hjIs9* [*ges-1p*::*glo-1*::GFP + *unc-119*(+)] was obtained from Caenorhabditis Genetic Center. To exclude unexpected additional mutations, mutant worms obtained were out-crossed 4 times. Males carrying mutations were generated from mutants and were used to transfer the mutation.

A set of oligonucleotides, UBXN6A-F and UBXN6A-R, UBXN6B-F and UBXN6B-R, UBXN6C-F and UBXN6C-R, UBXN6D-F and UBXN6D-R, UBXN6F-F and UBXN6F-R, UBXN6G-F and UBXN6G-R, and UBXN6I-F and UBXN6I-R, was annealed, and inserted into the *BsaI*-digested pMB70 vector, yielding pCKX1406, pCKX1407, pCKX1408, pCKX1409, pCKX1414, pCKX1415, and pCKX1417, respectively. To make a *ubxn-6* deletion strain, a mixture of plasmids, *Peft-3*::*cas9*-SV40_NLS::*tbb-2* 3'UTR (25 ng/μl), pCKX1409 (50 ng/μl), pCKX1414 (50 ng/μl), and pPD136.64 (25 ng/μl) was microinjected into the gonad of the wild-type N2 strain. Plasmids *Peft-3*::*cas9*-SV40_NLS::*tbb-2* 3'UTR [21] and pMB70 [22] were obtained from Addgene. The *Peft-3*::*cas9*-SV40_NLS::*tbb-2* 3'UTR plasmid produces the Cas9 enzyme [21]. pPD136.64 produces the YFP protein in the body wall muscle cells and was used as an injection marker [23]. YFP-positive F1 progenies were selected and their genomic DNA was analyzed for the deletion of the *ubxn-6* gene by PCR with primers UBXN6Fw-2 and UBXN6Rv-2. F2 progenies of the candidates were analyzed again, and the strains containing homogenic deletion of the *ubxn-6* gene were isolated. To exclude unexpected additional mutations including off-target mutations, mutant worms obtained were out-crossed 4 times. We therefore established the strain KXK1001 *ubxn-6* (*zye1001*).

Genomic DNA fragments containing the upstream region of *ubxn-6* and the entire *ubxn-6* gene were cloned onto the pBluescript II SK (+) vector using Gibson Assembly Master Mix (New England Biolabs), yielding pCKX1425. Therefore, the DNA fragment encoding V5-tag sequence was simultaneously inserted at the 5′ end of the *ubxn-6* gene. To avoid the possibility that Cas9 digests the template DNA, the sites on pCKX1425 recognized by sgRNAs produced from pCKX1414 and pCKX1417 were site-directed mutagenized by using the QuikChange II Site-Directed Mutagenesis Kit (Agilent Technologies), yielding pCKX1428. To make the V5-tag-inserted strain, a mixture of plasmids, *Peft-3*::*cas9*-SV40_NLS::*tbb-2* 3'UTR (25 ng/μl), pCKX1414 (50 ng/μl), pCKX1417 (50 ng/μl), pCKX1428 (100 ng/μl), and pPD136.64 (25 ng/μl) was microinjected into the gonad of the wild-type N2 strain. YFP-positive F1 progenies were selected. The portion of their genomic DNA was amplified by PCR with primers UBXN6upPCR and UBXN6downPCR, and digested with *XbaI*, whose recognition sequence exists in the sequence encoding V5-tag. F2 progenies of the candidates were analyzed again, and the strains containing homogenic insertion of the V5-tag encoding sequence were isolated. After 4-times outcross, we established the strain KXK1009.

DNA sequences of the constructed plasmids and strains were verified by DNA sequencing. Plasmid DNA was column purified by using the Wizard Plus SV Minipreps DNA Purification System (Promega) and filtered by using SUPREC-01 (TaKaRa). Primers used in this study were listed in Supplementary Table 1.

2.2. Preparation of anti-UBXN-6 antibody

The entire sequence encoding UBXN-6 was amplified by PCR with a cDNA clone yk1159e09 as a template, and primers ubxn6-Cold-5 and ubxn6-Cold-3, and cloned onto pCold I, yielding pMUR7. *Escherichia coli* BL21(DE3) was transformed with pMUR7. His-tagged UBXN-6 was overexpressed by temperature shift-down and the addition of 1 mM isopropyl-1-thio-β-D-galactopyranoside and purified by using HisTrap HP and HiTrap Q columns (GE Healthcare). Purified His-tagged UBXN-6 was pooled and used for development of antibody. Rabbit anti-UBXN-6 antisera was developed by IWAKI&CO., LTD. and purified using antigen-conjugated affinity resin.

2.3. Western blotting

Total lysates of worms were resolved on 10% SDS-PAGE gels, and then proteins were transferred to a nitrocellulose membrane. Prestained Protein Markers (Broad Range) (NACALAI TESQUE, INC.) or Dr. Western (Oriental Yeast CO., LTD.) was used as a Western blotting marker. Signals were detected with anti-UBXN-6 (1:1000), anti-GFP (Clontech; 1:1000), anti-UFD-2 (1:1000), anti-UFD-3 (1:1000), anti-V5 (MBL; 1:1000), and anti-α-tubulin (Sigma; 1:1000) antibodies as a primary antibody. Secondary antibodies were anti-mouse IgG horseradish peroxidase–conjugated F(ab')2 fragment (GE Healthcare; 1:5000) and anti-rabbit IgG horseradish peroxidase–conjugated F(ab')2 fragment (GE Healthcare; 1:5000). Proteins were visualized using Western Lightning Chemiluminescence Reagent Plus (Perkin–Elmer Life Sciences). Chemiluminescent signals were detected and quantified with LAS-4000 mini. α-Tubulin was used as a loading control.

2.4. Lifespan and brood size analyses

Lifespan assays were performed as described in Tsuda et al. [24]. Lifespan assays were repeated at least two times. We did not count worms that died due to internal hatching or crawling up the plate wall. Data analysis was performed as described by Han et al. [25], by using the publicly available analysis suite OASIS 2 (Online Application for Survival Analysis 2) (https://sbi.postech.ac.kr/oasis2/).

Brood size measurement was performed as described in Sasagawa et al. [26].

2.5. Treatment with tunicamycin and rapamycin and treatment of starvation

Worms were synchronously grown to the young adult and treated with tunicamycin (10 μg/ml) and rapamycin (100 μM) for 6 h.

For starvation assays, worms were synchronously grown to the young adult, and harvested, washed and incubated in NGM plates without *E. coli* OP50 for 12 h.

2.6. Confocal microscopic observation

Worms were mounted on 2% agar pad containing 10 mM levamisole and images were obtained using Leica TCS SP8 laser scanning confocal microscope. Confocal microscopic observation was performed as described previously [27]. Z-stack images were acquired at 0.8 μm slice interval at 40x/1.30 oil objective. The Z-position was selected from the surface of intestine to where intestinal lumen could be seen clearly. GFP excitation/emission was set to 493/517 nm to eliminate background autofluorescence [27]. The elimination of autofluorescence was confirmed by comparing intensities of the images taken at GFP excitation/emission 493/

578 nm and 493/517 nm, using the wild-type and *ubxn-6* deletion strains without the transgenic GFP construct.

3. Results and discussion

3.1. Construction of the ubxn-6 deletion mutant in C. elegans

UBXN-6 is unique, since it can bind to the N domain as well as the C-terminal portion of CDC-48 [8]. However, the *C. elegans ubxn-6* mutant has not been obtained and characterized so far. By using the CRISPR-Cas9 system, we first tried to create the *ubxn-6* deletion strain. It has been reported that the use of dual sgRNAs works efficiently to generate gene knockout mutations in *C. elegans* [28]. It has also been reported that the design of sgRNAs with a GG motif at the 3′ end of their protospacer sequences caused a high efficiency of targeted mutagenesis [29]. Therefore, we combined these two strategies to generate the targeted deletion mutation in the *ubxn-6* gene. As shown in Fig. 1, when both sgRNAs contained the GG sequence at the 3′ end of the protospacer sequences, a highly efficient introduction of the deletion mutation was occurred, although their deletion size was varied strain to strain. One of the mutants obtained contained a 1305bp deletion as shown in Fig. 1A and was used throughout this study. By contrast, when an sgRNA contained the A or T residue at the 3′ end of the protospacer sequence, efficiency was greatly reduced (Fig. 1). These results strongly indicated that the use of dual sgRNAs, which were designed with a GG motif at the 3' end of their protospacer sequences, worked very efficiently to generate the deletion mutations in *C. elegans*. By using a similar strategy, we also obtained the knock-in derivative of the V5-tag sequence at the N-terminal end of UBXN-6. Details were described in Materials and Methods.

To verify deletion and knock-in mutations at the protein level, we generated the anti-UBXN-6 antibody and performed Western blotting analyses. UBXN-6 is composed of 437 amino acid residues and its estimated molecular mass is 49.0 kDa. A band at the approximately 55.0 kDa position of the wild-type strain was missing in the *ubxn-6* mutant and its mobility was slightly decreased in the V5::UBXN-6-expressing knock-in strain (Fig. 1D

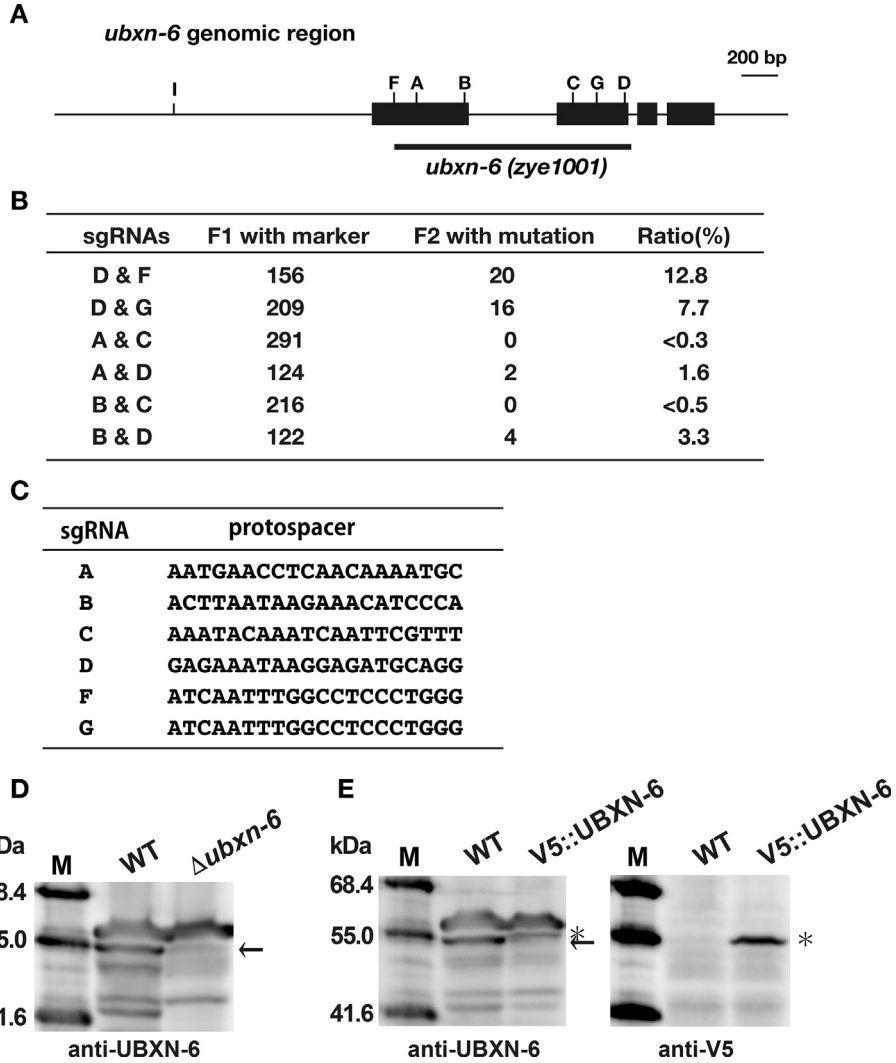

sgRNAs	F1 with marker	F2 with mutation	Ratio(%)
D & F	156	20	12.8
D & G	209	16	7.7
A & C	291	0	<0.3
A & D	124	2	1.6
B & C	216	0	<0.5
B & D	122	4	3.3

sgRNA	protospacer
A	AATGAACCTCAACAAAATGC
B	ACTTAATAAGAAACATCCCA
C	AAATACAAATCAATTCGTTT
D	GAGAAATAAGGAGATGCAGG
F	ATCAATTTGGCCTCCCTGGG
G	ATCAATTTGGCCTCCCTGGG

Fig. 1. Generation of the *ubxn-6* deletion mutant in *C. elegans*.
(A) The *ubxn-6* genomic region is schematically shown. Boxes represent exons for *ubxn-6* (exon-1 to −4 from the left). Positions of the recognition sites by sgRNAs are also indicated. The region of deletion in the *ubxn-6* deletion mutant is indicated with a thick bar. (B) Summary of dual sgRNA experiments. Number of transgenic F1 and mutant F2 progeny are shown. (C) Protospacer sequences for each sgRNA are shown. (D) Total lysates of the wild-type and *ubxn-6* deletion strains were analyzed by Western blotting using the anti-UBXN-6 antibody. Molecular sizes are indicated to the left of the panel. The position of UBXN-6 is indicated with an arrow to the right of the panel. (E) Total lysates of the wild-type and V5::UBXN-6-expressing strains were analyzed by Western blotting using the anti-UBXN-6 and anti-V5 antibodies. The positions of UBXN-6 and V5::UBXN-6 are indicated with an arrow and an asterisk, respectively, to the right of the panel.

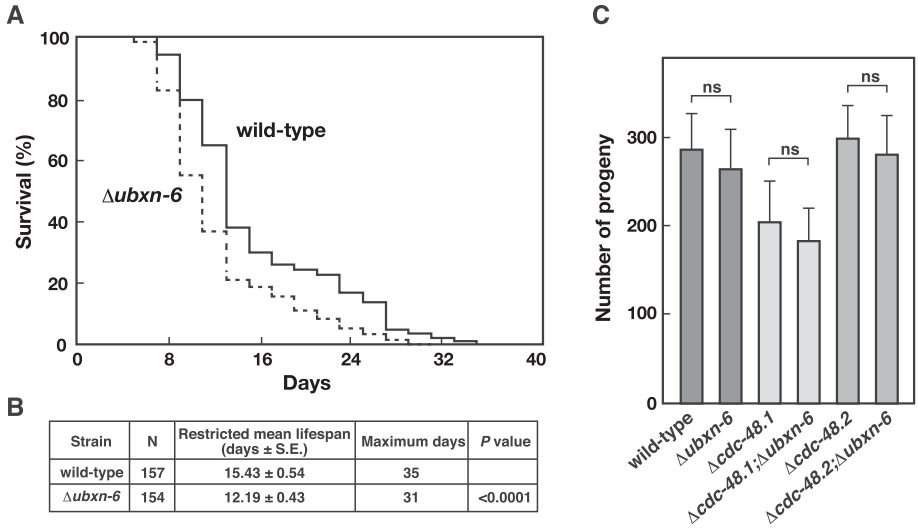

B

Strain	N	Restricted mean lifespan (days ± S.E.)	Maximum days	*P* value
wild-type	157	15.43 ± 0.54	35	
Δ*ubxn-6*	154	12.19 ± 0.43	31	<0.0001

Fig. 2. Effects of the *ubxn-6* deletion mutation on lifespan and brood size.
(A) More than 100 worms of the wild-type and *ubxn-6* deletion strains were used to investigate worm lifespan. The data were processed via Kaplan-Meir survival analysis of OASIS 2 (https://sbi.postech.ac.kr/oasis2). (B) Restricted mean lifespans, maximum days, and *P* values are shown for each strain. (C) Brood size of wild-type, Δ*ubxn-6*, Δ*cdc-48.1*, Δ*cdc-48.1*; Δ*ubxn-6*, Δ*cdc-48.2*, Δ*cdc-48.2*; Δ*ubxn-6* strains were measured. Results are mean of at least ten animals. Error bars indicate standard deviation. Statistical significance was assessed by Student's *t*-test: ns, not significant.

and E). These results indicate that the band with the 55.0 kDa molecular size is UBXN-6 and that its deletion was successfully confirmed in the *ubxn-6* mutant.

3.2. Physiological characterization of the ubxn-6 mutant

We first analyzed the lifespan and brood size of the *ubxn-6* mutant. The lifespan of the *ubxn-6* mutant was shorter than that of the wild-type strain (Fig. 2A and B). The brood size of the *ubxn-6* mutant was similar with that of the wild-type strain (Fig. 2C). Previously, we reported that the *cdc-48.1* mutant, but not the *cdc-48.2* mutant showed the decreased brood size at 20 °C [26]. The ratio of the amount of CDC-48.1 and CDC-48.2 is 2 to 1 [11]. The *ubxn-6* deletion was introduced into these mutants to prepare double mutants: *cdc-48.1*; *ubxn-6* and *cdc-48.2*; *ubxn-6*. The introduction of the *ubxn-6* deletion mutation did not affect the brood size independently of the amount of CDC-48 proteins, suggesting that UBXN-6 may not be involved in the process of the

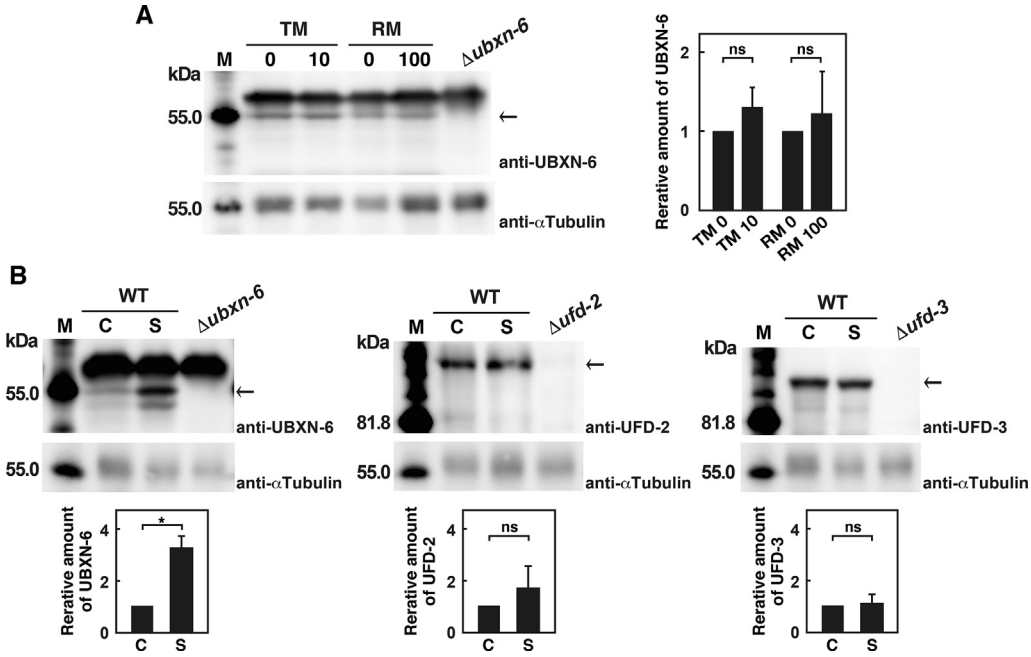

Fig. 3. Effects of drugs and stress treatment on the amount of UBXN-6.
Wild-type worms were treated with tunicamycin (TM: 0 and 10 μg/ml) and rapamycin (RM: 0 and 100 μM) for 6 h (A) and with starvation for 12 h (C: control, S: starvation) (B). The *ubxn-6*, *ufd-2* and *ufd-3* deletion strains were used as a negative control. Total lysates were analyzed by Western blotting using the anti-UBXN-6, anti-UFD-2, anti-UFD-3 and anti-α-tubulin antibodies. α-Tubulin was used as a loading control. Molecular sizes are indicated to the left of the panel. The position of UBXN-6, UFD-2 or UFD-3 is indicated with an arrow to the right of the panel. We performed three independent experiments and similar results were obtained in each experiment. Error bars indicate standard deviation. Statistical significance was assessed by Student's *t*-test: *, $P < 0.001$; ns, not significant.

brood size determination. Alternatively, another cofactor may take care of it.

3.3. UBXN-6 is induced upon starvation

Based on the previous reports, UBXN-6 might be involved in the endoplasmic reticulum-associated degradation (ERAD), autophagy or the endosome-lysosome trafficking [12–16]. We then analyzed whether the amount of UBXN-6 is affected by the treatment with tunicamycin and rapamycin, which are inducers of ERAD and autophagy, respectively. Young adult worms were treated with the drugs and analyzed by Western blotting with the anti-UBXN-6 antibody. As shown in Fig. 3A, the amount of UBXN-6 was not changed upon exposure to these drugs, suggesting that the physiological level of UBXN-6 might be enough to properly maintain ERAD and autophagy in *C. elegans*. On the other hand, it is interesting to mention that the amount of UBXN-6 was approximately 3-fold increased upon starvation (Fig. 3B). Importantly, the induction upon starvation was specific to UBXN-6, but not for other C-terminal cofactors UFD-2 and UFD-3 (Fig. 3B).

3.4. UBXN-6 is necessary for lysosomal clearance upon starvation

Since starvation causes the important alterations in intracellular signaling and membrane trafficking [30], the induction of UBXN-6 might be necessary for rapid turnover of cellular materials upon starvation in *C. elegans*. *C. elegans* intestine is an excellent model for membrane trafficking and lysosome biogenesis studies. Therefore, we examined the fate of GLO-1 protein, which is a lysosome-related protein and can be used as a marker for the endosome-lysosome trafficking [31]. GLO-1::GFP that was expressed in intestine under the control of the *ges-1* promoter was monitored upon starvation by confocal microscopy. Before starvation, GLO-1::GFP proteins were highly expressed and dispersed in intestine, and very few GLO-1::GFP was enriched in punctate structures within the intestinal cells (Fig. 4A). No significant difference was found in GLO-

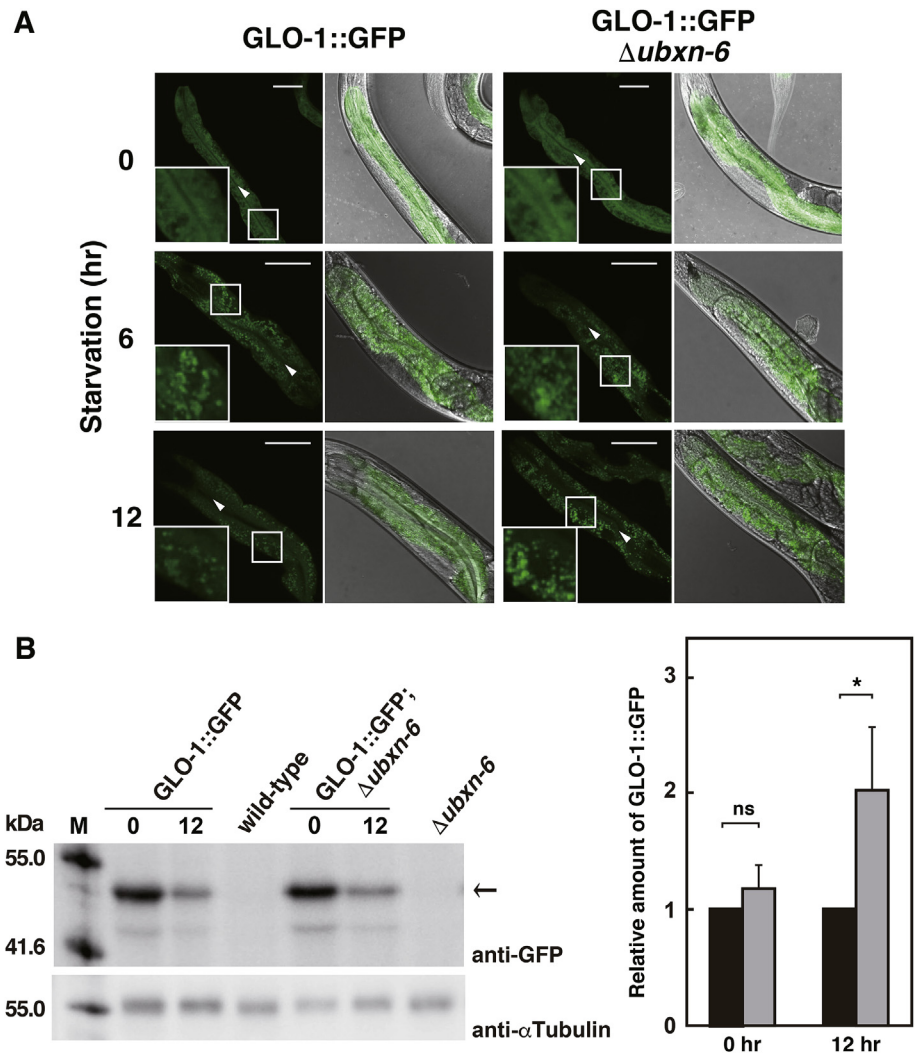

Fig. 4. Effects of starvation on the GLO-1::GFP localization and accumulation.
(A) GLO-1::GFP-expressing wild-type and *ubxn-6* deletion strains were treated with starvation for 0, 6 and 12 h and observed by a confocal microscope. Fluorescent image (left) and merged image with fluorescent and DIC (right) are shown for each sample. Inlets represent enlarged images. Arrowhead: intestinal lumen. Bar: 50 μm (B) GLO-1::GFP-expressing wild-type and *ubxn-6* deletion strains were treated with starvation for 0 and 12 h. The wild-type and *ubxn-6* deletion strains were used as a negative control. Total lysates were analyzed by Western blotting using the anti-GFP and anti-α-tubulin antibodies. α-Tubulin was used as a loading control. Molecular sizes are indicated to the left of the panel. The position of GLO-1::GFP is indicated with an arrow to the right of the panel. We performed three independent experiments and similar results were obtained in each experiment. Black bar and gray bar indicate GLO-1::GFP and GLO-1::GFP; Δ*ubxn-6*, respectively. Error bars indicate standard deviation. Statistical significance was assessed by Student's *t*-test: *, $P < 0.001$; ns, not significant.

1::GFP distribution between the wild-type and *ubxn-6* deletion strains in the well-fed condition (Fig. 4A). After 6 h starvation, the diffusion of GLO-1::GFP was largely reduced and GLO-1::GFP was mainly found in foci. When starvation progress, the number of GLO-1::GFP foci was reduced after 12 h starvation in wild-type (Fig. 4A). These results are consistent with the previous reports that in short period of starvation time, endocytosis and lysosomal activity were upregulated, and the number and size of lysosomal structures were dramatically increased due to increased fusion of lysosome with autophagosomes, but lysosome size and number were recovered in longer starvation time [30,32,33]. In contrast, the number of GLO-1::GFP foci was remained more in the *ubxn-6* mutant after 12 h starvation comparing with wild-type (Fig. 4A), which indicated that endosome-lysosome trafficking became slowdown and lysosomal clearance was delayed in the *ubxn-6* mutant. We then carried out Western blotting to measure the amount of GLO-1::GFP. We found that the amount of GLO-1::GFP was slightly but significantly higher in the *ubxn-6* mutant than that in the wild-type strain after 12 h starvation (Fig. 4B). These results suggested that UBXN-6 might be involved in the endosome-lysosome trafficking system-mediated clearance upon starvation and that the endosome and/or lysosome foci might be accumulated in the *ubxn-6* mutant. Our results are consistent with the previous reports that UBXD1 is involved in modulating the trafficking of ERGIC-53-containing vesicles [12] and endo-lysosomal sorting of ubiquitinated CAV1 [13].

3.5. Perspective

It should be noted that UBXD1 was defective to bind to p97 with mutations found in familial IBMPFD (Inclusion Body Myopathy with Paget's disease and Frontotemporal Dementia) and ALS (Amyotrophic Lateral Sclerosis) diseases [13]. Disease-associated mutations in p97 or siRNA-mediated depletion of UBXD1 interfered with the CAV1 trafficking by blocking of CAV1 transport to endolysosome [13]. Moreover, abnormalities in both endosome and lysosome or dysregulation in their trafficking were linked to numerous neurodegenerative diseases such as Alzheimer's disease, Parkinson's disease and Lewy body dementia [34–36]. So, delayed clearance of cellular components by lysosome in the *ubxn-6* mutant upon starvation may be linked to the disease pathogenesis. Therefore, the *ubxn-6* deletion strain of *C. elegans* can be used for studying pathophysiology of neurodegenerative disease, although the precise mechanism of UBXN-6 involvement in endolysosomal trafficking upon starvation remains elusive.

Conflicts of interest

The authors declare no conflict of interest.

Acknowledgments

We are grateful to the Caenorhabditis Genetic Center and Dr. Shohei Mitani (Tokyo Women's Medical University) for *C. elegans* strains and Dr. Yuji Kohara (National Institute of Genetics) for *C. elegans* cDNA clones. This work was supported by the Program for Leading Graduate Schools HIGO (Health life science: Interdisciplinary and Glocal Oriented) from MEXT, Japan and in part by Grants-in-Aid for Scientific Research (B) (#16H04764 to T.O.) and for Scientific Research (C) (#16K08594 to K.Y.) from the Japan Society for the Promotion of Science.

Appendix A. Supplementary data

Supplementary data to this article can be found online at https://doi.org/10.1016/j.bbrc.2018.12.155.

References

[1] J. van den Boom, H. Meyer, VCP/p97-mediated unfolding as a principle in protein homeostasis and signaling, Mol. Cell 69 (2017) 182–194.
[2] G.H. Baek, H. Cheng, V. Choe, X. Bao, J. Shao, S. Luo, H. Rao, Cdc48: a swiss army knife of cell biology, J. Amino Acids 2013 (2013) 183421.
[3] H. Meyer, M. Bug, S. Bremer, Emerging functions of the VCP/p97 AAA-ATPase in the ubiquitin system, Nat. Cell Biol. 14 (2012) 117–123.
[4] K. Yamanaka, Y. Sasagawa, T. Ogura, Recent advances in p97/VCP/Cdc48 cellular functions, Biochem. Biophys. Acta 1823 (2012) 130–137.
[5] S. Rumpf, S. Jentsch, Functional division of substrate processing cofactors of the ubiquitin-selective Cdc48 chaperone, Mol. Cell 21 (2006) 261–269.
[6] P. Hanzelmann, H. Schindelin, The interplay of cofactor interactions and post-translational modifications in the regulation of the AAA+ ATPase p97, Front. Mol. Biosci. 13 (2017) 21.
[7] A. Buchberger, H. Schindelin, P. Hanzelmann, Control of p97 function by cofactor binding, FEBS Lett. 589 (2015) 2578–2589.
[8] Y. Sasagawa, K. Yamanaka, Y. Saito-Sasagawa, T. Ogura, *Caenorhabditis elegans* UBX cofactors for CDC-48/p97 control spermatogenesis, Gene Cell. 15 (2010) 1201–1215.
[9] Y. Murayama, T. Ogura, K. Yamanaka, Characterization of C-terminal adaptors, UFD-2 and UFD-3, of CDC-48 on polyglutamine aggregation in *C. elegans*, Biochem. Biophys. Res. Commun. 459 (2015) 154–160.
[10] K. Yamanaka, Y. Okubo, T. Suzaki, T. Ogura, Analysis of the two p97/VCP/Cdc48p proteins of *Caenorhabditis elegans* and their suppression of polyglutamine-induced protein aggregation, J. Struct. Biol. 146 (2004) 242–250.
[11] S. Yamauchi, K. Yamanaka, T. Ogura, Comparative analysis of expression of two p97 homologues in *Caenorhabditis elegans*, Biochem. Biophys. Res. Commun. 345 (2006) 746–753.
[12] D.S. Haines, J.E. Lee, S.L. Beauparlant, D.B. Kyle, W. den Besten, M.J. Sweredoski, R.L. Graham, S. Hess, R.J. Deshaies, Protein interaction profiling of the p97 adaptor UBXD1 points to a role for the complex in modulating ERGIC-53 trafficking, Mol. Cell. Proteomics 11 (2012). M111.016444.
[13] D. Ritz, M. Vuk, P. Kirchner, M. Bug, S. Schutz, A. Hayer, S. Bremer, C. Lusk, R.H. Baloh, H. Lee, T. Glatter, M. Gstaiger, R. Aebersold, C.C. Weihl, H. Meyer, Endolysosomal sorting of ubiquitylated caveolin-1 is regulated by VCP and UBXD1 and impaired by VCP disease mutations, Nat. Cell Biol. 13 (2011) 1116–1123.
[14] C. Papadopoulos, P. Kirchner, M. Bug, D. Grum, L. Koerver, N. Schulze, R. Poehler, A. Dressler, S. Fengler, K. Arhzaouy, V. Lux, M. Ehrmann, C.C. Weihl, H. Meyer, VCP/p97 cooperates with YOD1, UBXD1 and PLAA to drive clearance of ruptured lysosomes by autophagy, EMBO J. 36 (2017) 135–150.
[15] X. Guo, X. Qi, VCP cooperates with UBXD1 to degrade mitochondrial outer membrane protein MCL in model of Huntington's disease, Biochem. Biophys. Acta 1863 (2017) 552–559.
[16] A.C. Bento, C.C. Bippes, C. Kohler, C. Hemion, S. Frank, A. Neutzner, UBXD1 is a mitochondrial recruitment factor for p97/VCP and promotes mitophagy, Sci. Rep. 8 (2018) 12415.
[17] L. Madsen, K.M. Andersen, S. Prag, T. Moos, C.A. Semple, M. Seeger, R. Hartmann-Petersen, Ubxd1 is a novel co-factor of the human p97 ATPase, Int. J. Biochem. Cell Biol. 40 (2008) 2927–2942.
[18] M. Kern, V. Fernandez-Saiz, Z. Schafer, A. Buchberger, UBXD1 binds p97 through two independent binding sites, Biochem. Biophys. Res. Commun. 380 (2009) 303–307.
[19] F. Trusch, A. Metena, M. Vuk, L. Koerver, H. Knavelsrud, P. Freemont, H. Meyer, P. Bayer, The N-terminal region of the ubiquitin regulatory X (UBX) domain-containing protein 1 (UBXD1) modulates interdomain communication within the valosin-containing protein p97, J. Biol. Chem. 290 (2015) 29414–29427.
[20] S. Brenner, The genetics of *Caenorhabditis elegans*, Genetics 77 (1974) 71–94.
[21] A.E. Friedland, Y.B. Tzur, K.M. Esvelt, M.P. Colaiacovo, G.M. Church, J.A. Calarco, Heritable genome editing in *C. elegans* via a CRISPR-Cas9 system, Nat. Methods 10 (2013) 741–743.
[22] S. Waaijers, V. Portegijs, J. Kerver, B.B.L.G. Lemmens, M. Tijsterman, S. van den Heuvel, M. Boxem, CRISPR/Cas9-targeted mutagenesis in *Caenorhabditis elegans*, Genetics 195 (2013) 1187–1191.
[23] A. Fire, S.W. Harrison, D. Dixon, A modular set of *lacZ* fusion vectors for studying gene expressing in *Caenorhabditis elegans*, Gene 93 (1990) 189–198.
[24] Y. Tsuda, K. Yamanaka, R. Toyoshima, M. Ueda, T. Masuda, Y. Misumi, T. Ogura, Y. Ando, Development of transgenic *Caenorhabditis elegans* expressing human transthyretin as a model for drug screening, Sci. Rep. 8 (2018) 17884.
[25] S.K. Han, D. Lee, H. Lee, D. Kim, H.G. Son, J.-S. Yang, S.-J.V. Lee, S. Kim, OASIS 2: online application for survival analysis 2 with features for the analysis of maximal lifespan and healthspan in aging research, Oncotarget 7 (2016) 56147–56152.
[26] Y. Sasagawa, M. Otani, N. Higashitani, A. Higashitani, K. Sato, T. Ogura, K. Yamanaka, *Caenorhabditis elegans* p97 controls germline-specific sex determination by controlling the TRA-1 level in a CUL-2-dependent manner, J. Cell Sci. 122 (2009) 3663–3672.
[27] J.Y. Chang, C. Kumsta, A.B. Hellman, L.M. Adams, M. Hansen, Spatiotemporal regulation of autophagy during *Caenorhabditis elegans* aging, eLife 6 (2017), e18495.
[28] X. Chen, F. Xu, C. Zhu, J. Ji, X. Zhou, X. Feng, S. Guang, Dual sgRNA-directed

gene knockout using CRISPR/Cas9 technology in *Caenorhabditis elegans*, Sci. Rep. 4 (2014) 7581.
[29] B. Farboud, B.J. Meyer, Dramatic enhancement of genome editing by CRISPR/Cas9 through improved guide RNA design, Genetics 199 (2015) 959–971.
[30] C.B. Jones, E.M. Ott, J.M. Keener, M. Curtiss, V. Sandrin, M. Babst, Regulation of membrane protein degradation by starvation-response pathways, Traffic 13 (2012) 468–482.
[31] G.J. Hermann, L.K. Schoeder, C.A. Hieb, A.M. Kershner, B.M. Rabbitts, P. Fonarev, B.D. Grant, J.R. Priess, Genetic analysis of lysosomal trafficking in *Caenorhabditis elegans*, Mol. Biol. Cell 16 (2005) 3273–3288.
[32] L. Yu, C.K. McPhee, L. Zheng, G.A. Mardones, Y. Rong, J. Peng, N. Mi, Y. Zhao, Z. Liu, F. Wan, D.W. Hailey, V. Oorschot, J. Klumperman, E.H. Baehrecke, M.J. Lenardo, Termination of autophagy and reformation of lysosomes regulated by mTOR, Nature 465 (2010) 942–946.
[33] W. Wang, Q. Gao, M. Yang, X. Zhang, L. Yu, M. Lawas, X. Li, M. Bryant-Genevier, N.T. Southall, J. Marugan, M. Ferrer, H. Xu, Up-regulation of lysosomal TRPML1 channels is essential for lysosomal adaptation to nutrient starvation, Proc. Natl. Acad. Sci. U.S.A. 112 (2015). E1373–1381.
[34] J. Tan, G. Evin, Beta-site APP-cleaving enzyme 1 trafficking and Alzheimer's disease pathogenesis, J. Neurochem. 120 (2012) 869–880.
[35] J. Wu, R.S. Petralia, H. Kurushima, H. Patel, M.Y. Jung, L. Volk, S. Chowdhury, J.D. Shepherd, M. Dehoff, Y. Li, D. Kuhl, R.L. Huganir, D.L. Price, R. Scannevin, J.C. Troncoso, P.C. Wong, P.F. Worley, Arc/Arg3.1 regulates an endosomal pathway essential for activity-dependent β-amyloid generation, Cell 147 (2011) 615–628.
[36] J. Neefjes, R. van der Kant, Stuck in traffic: an emerging theme in diseases of the nervous system, Trends Neurosci. 37 (2014) 66–76.

Supplementary Table S1. Oligonucleotide primers used in this study.

Primer name	Sequence (5' to 3')
UBXN6A-F	AATTAATGAACCTCAACAAAATGC
UBXN6A-R	AAACGCATTTTGTTGAGGTTCATT
UBXN6B-F	AATTACTTAATAAGAAACATCCCA
UBXN6B-R	AAACTGGGATGTTTCTTATTAAGT
UBXN6C-F	AATTAAATACAAATCAATTCGTTT
UBXN6C-R	AAACAAACGAATTGATTTGTATTT
UBXN6D-F	AATTGAGAAATAAGGAGATGCAGG
UBXN6D-R	AAACCCTGCATCTCCTTATTTCTC
UBXN6F-F	AATTATCAATTTGGCCTCCCTGGG
UBXN6F-R	AAACCCCAGGGAGGCCAAATTGAT
UBXN6G-F	AATTACCATCAGATGTTCATTTGG
UBXN6G-R	AAACCCAAATGAACATCTGATGGT
UBXN6I-F	AATTGGAGTGCACAGAAAAGTGGG
UBXN6I-R	AAACCCCACTTTTCTGTGCACTCC
UBXN6Fw-2	GAGTCATCTTCGCAGCCTTC
UBXN6Rv-2	CAAGCTCCTGGATAATTTCG
UBXN6F-mutF	CTGCCCACGCTGGAGCTGCTCAGGGAGGCCAAATTG
UBXN6F-mutR	CAATTTGGCCTCCCTGAGCAGCTCCAGCGTGGGCAG
UBXN6I-mutF	GGAGTGCACAGAAAAGTGTGCGAGGTTTGCTATCGCAAGAG
UBXN6I-mutR	CTCTTGCGATAGCAAACCTCGCACACTTTTCTGTGCACTCC
ubxn6-Cold-5	CCGACTCGAGATGAAAGTTTTCTCGTTG
ubxn6-Cold-3	CCGACTCGAGTTACAGTTCATCATGATCC